Available online at www.sciencedirect.com
ScienceDirect
Thermochimica Acta 470 (2008) 91–97
thermochimica acta
www.elsevier.com/locate/tca

Thermal decomposition of praseodymium acetate as a precursor of praseodymium oxide catalyst

B.M. Abu-Zied*, S.A. Soliman

Chemistry Department, Faculty of Science, Assiut University, 71516 Assiut, Egypt

Received 9 September 2007; received in revised form 30 January 2008; accepted 7 February 2008
Available online 15 February 2008

Abstract

Thermal events encountered throughout the heat treatment of praseodymium acetate, $Pr(CH_3COO)_3{\cdot}H_2O$, were studied in nitrogen and air atmospheres. The samples calcined at the 300–700 °C temperature range were characterized using XRD, IR and N_2 adsorption. Moreover, in situ electrical conductivity was employed to follow up the formation of the different decomposition intermediates. The results indicated that the anhydrous salt decomposes to the final product, $PrO_{1.833}$, through the formation of the following intermediates: $Pr(OH)(CH_3COO)_2$, $PrO(CH_3COO)$ and $Pr_2O_2(CO_3)$. $PrO_{1.833}$ formed at 500, 600, and 700 °C possesses a surface area of 17, 16 and 10 m^2/g and crystallites size of 14, 17 and 30 nm, respectively.

Keywords: Praseodymium acetate; Praseodymium oxide; Thermal analysis; XRD

1. Introduction

Praseodymium oxides comprise stoichiometric, Pr_2O_3 and PrO_2, as well as non-stoichiometric oxides, PrO_x ($x = 1.833$, 1.810, 1.780, 1.714 and 1.67) [1–4]. Stoichiometric oxides adopt hexagonal, Pr_2O_3, and fluorite, PrO_2, structures whereas non-stoichiometric ones are oxygen-deficient modifications of the fluorite structure [1–4]. Praseodymium oxide $PrO_{1.833}$ (or Pr_6O_{11}) is usually produced via the thermal decomposition of many salts such as acetate [1,5], oxalate [2,4], formate [6], nitrate [7], adipate and sebacate [8], and citrate [3]. In this context, it was reported that $PrO_{1.833}$ formed from the acetate precursor has a higher surface area than that obtained from oxalate one [1].

Pr_6O_{11} is known to be utilized in the production of inorganic pigments. High-temperature calcinations of Pr_6O_{11} and CeO_2 produce $Pr_xCe_{1-x}O_2$ pigment which gives interesting color hues in ceramic glazes [9]. As a catalyst, Pr_6O_{11} exhibits good activity performance during the oxidative coupling of methane [10]. C_2H_4 selectivity was enhanced by the presence of tetrachloromethane as a feed-stream additive and/or on loading $PrCl_3$ on Pr_6O_{11}. Parallel to that work, Asami et al. [11] showed that praseodymium oxide, Pr_6O_{11}, exhibits the highest yield for the synthesis of ethane and ethylene from methane and carbon dioxide. Earlier investigation of Hussein [2] has pointed out that Pr_6O_{11} is highly active towards isopropanol decomposition. However, propylene selectivity was found to be lower compared to that of Pr_2O_3, because of the lower acidity of Pr_6O_{11} [2]. More recently, it was shown that incorporation of praseodymium oxide into ceria–zirconia yielding Ce–Zr–Pr–O solid solution which exhibit good activity for soot oxidation [12].

Thermal decomposition of praseodymium acetate has been studied briefly. Hussein [1] and Shaplygin et al. [5] reported that the first step in the decomposition pathway is the dehydration giving the anhydrous salt. Like many other rare earth carboxylates [2–4,6,8,13–17], the thermal decomposition proceeds via the formation of oxycarbonate as intermediate leading eventually to the formation of the metal oxide. Here, however, Hussein suggested that the formation of praseodymium oxycarbonate follows the formation of another intermediate, $PrO(CH_3COO)$ [1]. Shaplygin group [5] proposed the formation of another intermediate, $Pr_2(CH_3COO)_4CO_3$. In both investigations there is a lack of information concerning the isothermal decomposition of this salt.

The existence of special fast transport paths (e.g. surfaces, pores, grain boundaries, etc.) for the decomposition of oxide

* Corresponding author. Tel.: +20 12 2942778; fax: +20 88 2342708.
E-mail addresses: babuzied@aun.edu.eg (B.M. Abu-Zied), sa_soliman@yahoo.com (S.A. Soliman).

0040-6031/$ – see front matter © 2008 Elsevier B.V. All rights reserved.
doi:10.1016/j.tca.2008.02.002

precursors eventually leads to materials possessing pores, lattice imperfections and other characteristics that are necessary for high surface reactivity [4]. The knowledge of all the intermediate stages of thermal dissociation of the given material provides a proper base for kinetic as well as mechanistic studies. This, in turn, provides better understanding of the conditions required to obtain a solid having a specific features. Previous results in the literature are encouraging, but further engagement is necessary to shed more light on the properties as well as the catalytic activity of praseodymium oxides. In our paper, we used praseodymium acetate as a precursor of praseodymium oxide catalyst. Thermal decomposition of this precursor, in air and nitrogen atmospheres, was studied using TGA, DTG, and DTA analyses. In addition, the thermal decomposition of this salt was studied isothermally. Moreover, in situ electrical conductivity measurements were used to follow up the various steps accompanying the thermal decomposition. Based on the thermal analysis results, the precursor was calcined at 300–700 °C temperature range. The obtained products were characterized using IR and XRD analyses. In addition, the texture of the produced solids was investigated using nitrogen adsorption.

2. Experimental

The praseodymium acetate, $Pr(CH_3COO)_3{\cdot}H_2O$, used was 99.9% pure (Strem Chemicals). Based on the thermal analysis results (vide infra) the parent salt, i.e. PrAc, was calcined at 300–700 °C, in air atmosphere, for 3 h. For simplicity, the calcination products will be referred to by abbreviations Pr-*x*, where *x* indicated the calcination temperature.

The simultaneous TGA, DTG and DTA curves were recorded with a Shimadzu DT-60 apparatus using a heating rate of 10 °C min^{-1} in air and nitrogen atmospheres. The average masses of the samples were 10 mg. α-Al_2O_3 was used as a reference in the DTA measurements. The study of the isothermal decomposition of praseodymium acetate was carried out at 225–400 °C temperature range. The in situ electrical conductivity measurements were carried out using a conductivity cell described by Chapman et al. [18]. The temperature was controlled with a WEMA temperature controller. The resistance measurements were carried out using a Keithley 610C solid-state electrometer. IR spectra of the different calcination products were performed by the KBr disc technique in the wavelength range 4000–500 cm^{-1}, using Shmadzu 470 infrared spectrophotometer. Surface areas, S_{BET}, were determined by BET analysis of the corresponding nitrogen adsorption isotherms (measured at −196 °C) [19]. The isotherms were obtained by using Quantachrome (Nova 3200 series) multi-gas adsorption apparatus. The S_t values were also obtained using the V_a−t plots of de Boer et al. [20]. Pore analysis was done according to Barrett–Joyner–Halenda (BJH) method [21]. X-ray diffraction patterns were recorded using a Philips diffractometer (type PW 103/00). The Philips generator, operated at 35 kV and 20 mA, provided a source of Cu Kα radiation. Average particle sizes were estimated from X-ray line width broadening using the Scherrer equation [22]:

$$\beta = \frac{K\lambda}{L_w \cos\theta} \quad (1)$$

where K is constant taken as 0.94 [23], λ is the X-ray wavelength and β is the corrected peak width. In these experiments, the width is taken as the full width at half maximum intensity of the peaks in the range 2θ = 25–32°.

3. Results and discussion

3.1. Thermal analysis and in situ electrical conductivity measurements

Fig. 1 depicts the TGA and DTG curves obtained for praseodymium acetate, PrAc, in dynamic atmospheres of nitrogen (a) and air (b) at a heating rate of 10 °C min^{-1}. In addition, thermogravimetric data and temperature intervals are summarized in Table 1. A close inspection of Fig. 1 reveals that, irrespective of the atmosphere utilized, heating the parent salt up to 900 °C is accompanied by six weight loss (WL) steps. These steps which are more resolved in nitrogen atmosphere are maximized at 71, 151, 290, 358, 405 and 519 °C. Taking into account the hygroscopic nature of this salt, the first WL (0.33%) could be assigned to the removal of adsorbed water. The second step brings a WL of 5.7% which is close to that

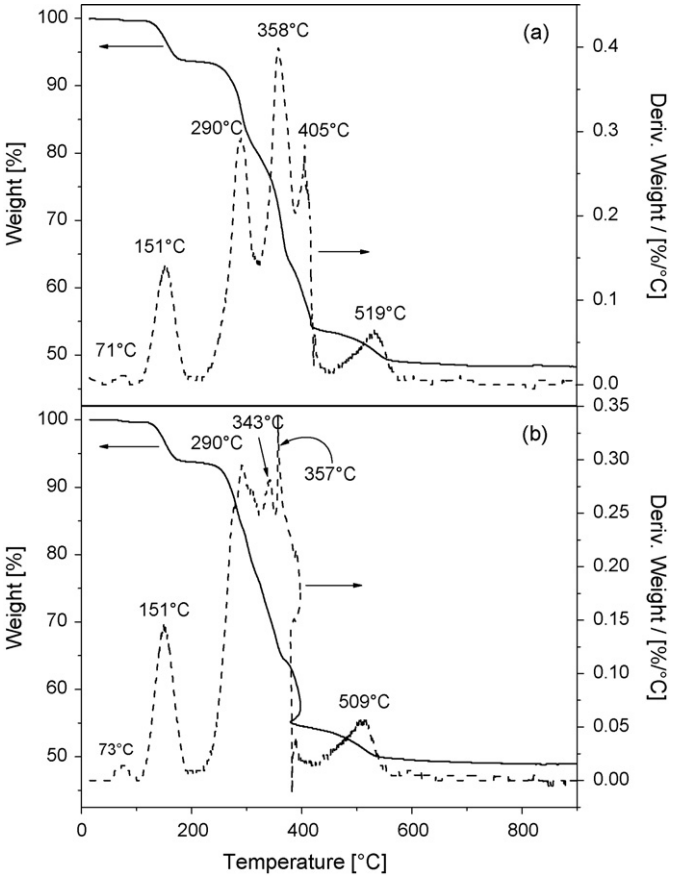

Fig. 1. TGA and DTG curves obtained by heating the parent praseodymium acetate in nitrogen (a) and air (b) atmospheres.

Table 1
Thermogravimetric data and temperature intervals in the thermal decomposition of praseodymium acetate, $Pr(CH_3COO)_3{\cdot}H_2O$

Decomposition stage	Temperature intervals (°C)	Weight loss (%)	
		Air	Nitrogen
I	40–100	0.38	0.33
II	100–200	5.86	5.70
III	200–305	13.11	12.95
IV	305–370	16.48	17.80
V	370–420	9.61	8.54
VI	420–650	5.25	4.89

(5.36%) anticipated to the removal of crystalline water. The third step is accompanied by a WL of 12.95% which is related to the start of the decomposition of the acetate anion. In this respect, Hussein [4] suggested that anhydrous PrAc decomposes firstly giving the hydroxy-acetate, $Pr(OH)(CH_3COO)_2$, intermediate, whereas Shaplygin group proposed the formation of $Pr_2(CH_3COO)_4(CO_3)$ intermediate [5]. These two intermediates are accompanied by 12.51% and 8.64% WL, respectively. Accordingly it seems that our results are in a good agreement with those reported by the first author. The hydroxy-acetate intermediate was proposed also for the decomposition of lanthanum [14], samarium [13], and thulium [15] acetates. Hence, one may write the following pathway:

$$Pr(CH_3COO)_{3(s)} \xrightarrow{290\,^{\circ}C} Pr(OH)(CH_3COO)_{2(s)} + CH_2{=}C{=}O_{(g)} \quad (2)$$

The formed ketene (CH_2=C=O), which was detected using in situ IR [13] and GC–MS spectroscopy [13,15], reacts readily with water molecule giving 1 mol of acetic acid according to [13,15,24]:

$$CH_2{=}C{=}O_{(g)} + H_2O_{(g)} \rightarrow CH_3COOH_{(g)} \quad (3)$$

The step maximized at 358 °C (Fig. 1a), i.e. step IV, is accompanied by 17.8% WL which matches satisfactorily with that (17.87%) expected for the removal of an acetic acid molecule according to

$$Pr(OH)(CH_3COO)_{2(s)} \xrightarrow{358\,^{\circ}C} PrO(CH_3COO)_{(s)} + CH_3COOH_{(g)} \quad (4)$$

The WL determined by the end of event V (8.54%) is close to that (8.64%) expected for the formation of dioxymonocarbonate as follows:

$$2PrO(CH_3COO)_{(s)} \xrightarrow{405\,^{\circ}C} Pr_2O_2(CO_3)_{(s)} + CH_3COCH_{3(g)} \quad (5)$$

The formation of $Pr_2O_2(CO_3)$ was confirmed using IR and XRD analyses for the sample calcined at 400 °C (vide infra). The final WL step, which maximized at 519 °C, proceeds via a 4.89% WL. Such value is close to that (4.96%) expected for the formation of $PrO_{1.833}$. The formation of $PrO_{1.833}$ and not Pr_2O_3 as a final decomposition product in both atmospheres suggests that the decomposition of $Pr_2O_2(CO_3)$ intermediate proceeds via the formation of a mixture of CO and CO_2. In agreement, it was reported that the thermal decomposition of

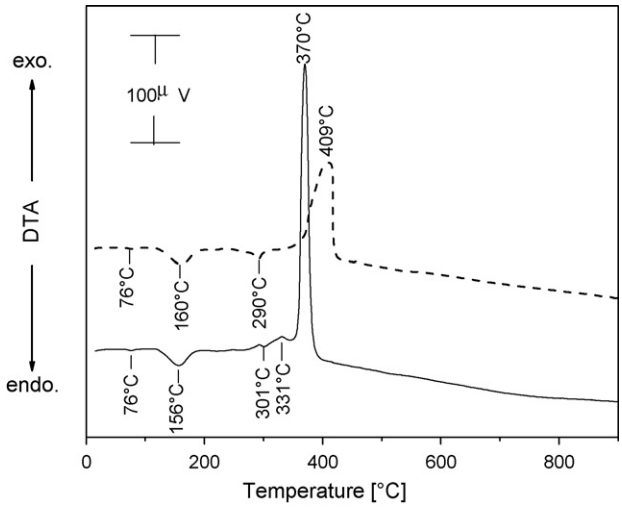

Fig. 2. DTA thermograms obtained by heating the praseodymium acetate parent till 900 °C in air (solid curve) and nitrogen (dashed curve) atmospheres.

praseodymium dioxymonocarbonate till 800 °C leads to the formation of $PrO_{1.833}$ only in air and nitrogen atmospheres [2]. The formation of Pr_2O_3 was obtained only in hydrogen atmosphere [2]. Moreover, the formation of Pr_2O_3 was also reported as a result of heating the acetate precursor in air at temperatures as high as 950 °C [5]. In this context, it is to be mentioned that the XRD analysis (vide infra) of the samples calcined at 500–700 °C range reveal the presence of $PrO_{1.833}$ as the only phase detected.

The DTA thermograms of PrAc heated in air and nitrogen atmospheres are shown in Fig. 2. From combining the data presented in Figs. 1 and 2 the following points can be raised: (i) the first two stages observed up on conducting the measurements in air atmosphere (Fig. 1b) are identical to those found in case of heating the parent salt in nitrogen (Fig. 1a). In this respect, DTA thermograms (Fig. 2) manifests that these steps are endothermic. (ii) The formation of $Pr(OH)(CH_3COO)_2$ intermediate in nitrogen atmosphere is accompanied by an endothermic effect at 290 °C. On conducting the measurements in air the formation of $Pr(OH)(CH_3COO)_2$ and $PrO(CH_3COO)$ intermediates proceeds via two consecutive steps maximized at 290 and 343 °C, respectively. In agreement, the reported work of Hussein [1] indicates that the anhydrous salt decomposes in air firstly via a 34.9% WL step. Such value is close to that (35.7%) anticipated to the $PrO(CH_3COO)$ intermediate formation. Accordingly, he suggested that the anhydrous salt decomposes directly to the oxyacetate intermediate. (iii) Steps IV and V, i.e. the formation of $PrO(CH_3COO)$ and $Pr_2O_2(CO_3)$ are exothermic in nature as shown by the two exothermic peaks located at 331 and 370 °C when the measurements were carried out in air and a broad peak extends from about 325 to 435 °C for the results obtained in nitrogen. Moreover, the high exothermicity of the peak maximized at 370 °C (Fig. 2) is reflected in the disturbance observed in the corresponding TGA thermogram (Fig. 1b) at the 350–400 °C temperature range. This could, also, be related to the combustion of the evolved organic gases accompanying the thermal treatment.

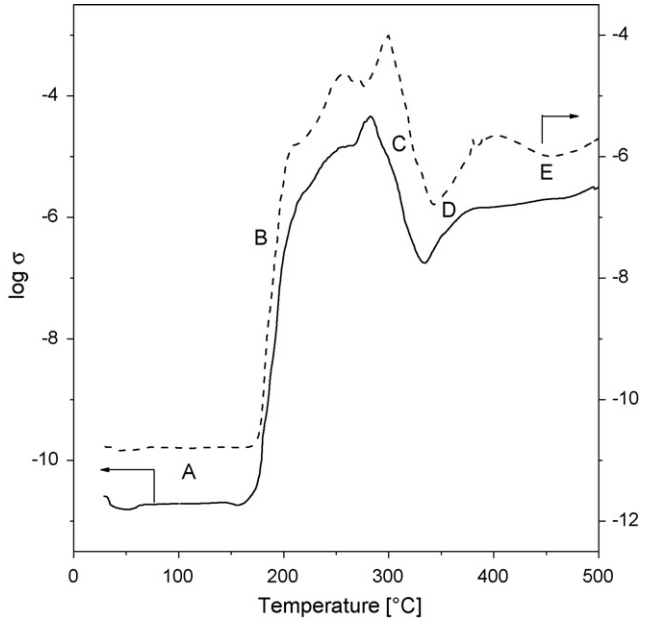

Fig. 3. Plot of log σ vs. temperature for praseodymium acetate during decomposition in air (—) and nitrogen (- - -) atmospheres.

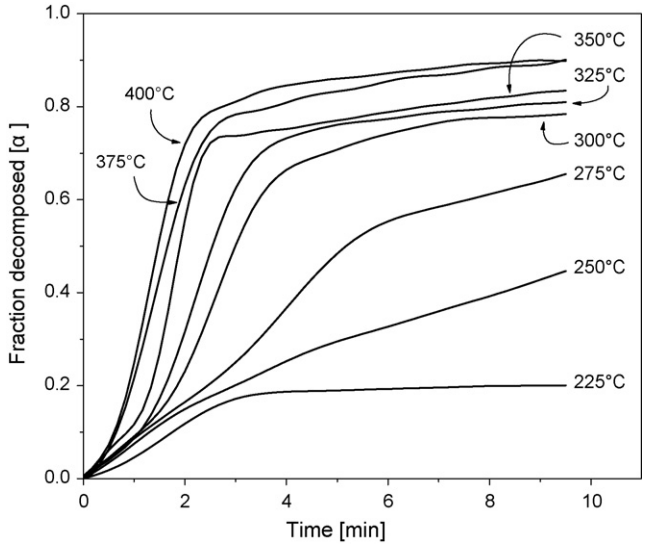

Fig. 4. Plot of fraction decomposed (α) vs. time (min) for the isothermal decomposition of praseodymium acetate in air atmosphere.

In situ electrical conductivity is an interesting tool for following up the phase changes occur during the heat treatment of solids. Combination of this tool with other tools such as thermal analysis, XRD, and IR gave a much more detailed view of the decomposition processes [25,26]. In situ electrical conductivity measurements were performed in nitrogen and air atmospheres. Fig. 3 illustrates the temperature dependence of electrical conductivity (σ) in both atmospheres. The value of σ remains nearly constant (region A) up to 145 and 160 °C in air and nitrogen atmospheres, respectively. Then it shows a steep increase till about 208 °C, followed by a steady increase, respectively, to 282 and 300 °C passing minima at 265 and 270 °C (region B). In this context, thermal analysis results (Figs. 1 and 2) revealed that the dehydration process, which maximized at 151 °C, was followed by the decomposition of the anhydrous acetate to the hydroxy-acetate (maximized at 290 °C). Hence, it seems that the dehydration did not bring a marked change in the electrical conductivity. On the other hand, the formation of the hydroxy-acetate is accompanied by an increase in the number of charge carriers, thus being responsible for the observed conductivity increase. Further heating of the parent salt up to 336 °C in air and 343 °C in nitrogen (region C) brings a continuous decrease in the electrical conductivity values. Such decrease could be related to the formation of $PrO(CH_3COO)$ at this temperature range. Raising the heating temperature to about 385 °C in air and 400 °C in nitrogen is associated with another increase in the measured conductivity values (region D). This increase can be assigned to the final decarboxylation process, i.e. the formation of dioxycarbonate intermediate. This suggestion is consistent with the fact that $Pr_2O_2(CO_3)$ is the only phase detected for the sample calcined, for 3 h in air, at 400 °C as indicated by infrared and X-ray diffraction analyses (vide infra). This finding copes with the work of Nikumbh group [26] who observed an increase in the σ values during the decarboxylation of copper and zinc malonate, maleate, and succinate complexes. In the final step (E), the σ values increases continuously in air, whereas in nitrogen it shows a mild decrease followed by a gradual increased till 500 °C (the temperature limit of our conductivity cell). This increase can be attributed to the formation of $PrO_{1.833}$ throughout the gradual decomposition of dioxycarbonate intermediate at the same temperature range. Here, again, the electrical conductivity measurement is in a good agreement with IR and XRD analysis where $PrO_{1.833}$ is the only phase detected at 500 °C.

3.2. Isothermal decomposition of PrAc

The rate of decomposition of praseodymium acetate was followed under isothermal conditions at 225–400 °C temperature range. The obtained data are plotted in Fig. 4 as the fraction of the reactant decomposed, α, versus time, t, with α defined as

$$\alpha = \frac{\Delta W}{\Delta W_{\max}} \tag{6}$$

where ΔW and $\Delta W_{\max}$ are the weight loss at time t and the maximum weight loss (assuming that the $PrO_{1.833}$ is the final product), respectively. It is evident that α–t curves are sigmoid in shape. The obtained values of α were 0.2 and 0.92 at 225 and 400 °C, respectively. It is of interest to supplement the isothermal measurements with some information gathered from structural characterization tools such as IR and XRD analyses. The holder of our TGA balance contain too little sample to make X-ray diffraction after recording the isothermal data. Therefore, the obtained residues were subjected to infrared analysis. Fig. 5 shows eight spectra recorded in the lattice vibration region (2000–500 cm^{-1}) where interesting information could be expected. The spectrum recorded for the sample heated at 225 °C ($\alpha = 0.2$) reveals the presence of the absorptions at 1600–500 cm^{-1}. These bands are located at 1570, 1440, 1345, (1053 and 1025), 953, 675, and 641 cm^{-1}. Such bands are assigned, respectively, to $\nu_{as}(COO^-)$, $\nu_s(COO^-)$, $\delta_s(CH_3)$,

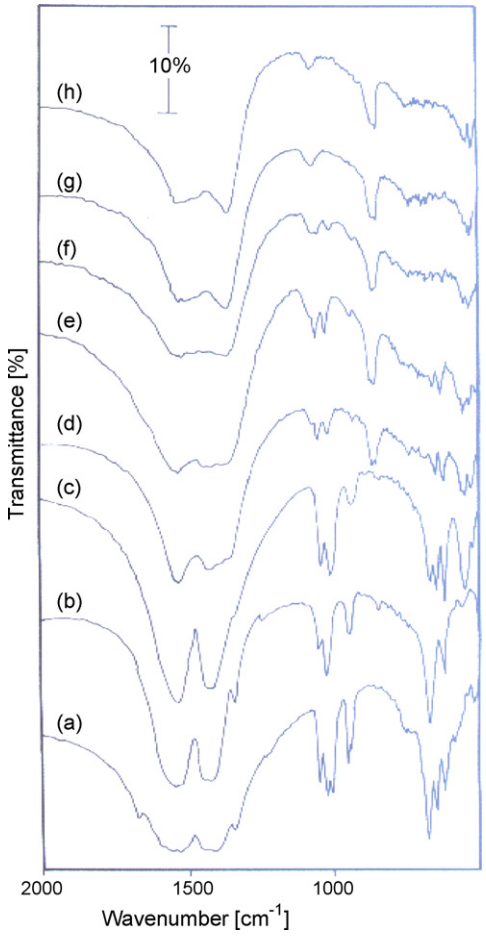

Fig. 5. IR spectra of the praseodymium acetate heated isothermally, 10 min in air, at 225 °C (a), 250 °C (b), 275 °C (c), 300 °C (d), 325 °C (e), 350 °C (f), 375 °C (g) and 400 °C (h).

$\rho(CH_3)$, ν(C–C), $\delta(COO^-)$, and $\pi(COO^-)$ vibration modes of acetate anions [1,13–15,27,28]. The IR spectra recorded for the samples heated up to 275 °C, i.e. till $\alpha = 0.68$ reveals the persistence of the above-mentioned vibrations, no other phases were detected. In this regard, it is worth noting that α value, 0.68, is close to that (0.72) expected for the oxy-acetate formation. A 25 °C raise in the measuring temperature, i.e. for the 300 °C treated sample, is accompanied by a decrease of the intensities belong to acetate anion vibrations and a disappearance of the band at around 670 cm^{-1} (due to $\delta(COO^-)$ mode). Meanwhile, new bands emerged at 1385 and 856 cm^{-1} which is assigned to carbonate oxide vibrations [14,15]. At this stage a value of $\alpha = 0.80$ was obtained. This lies between that expected for $PrO(CH_3COO)$, $\alpha = 0.72$, and for $Pr_2O_2(CO_3)$, $\alpha = 0.90$. Accordingly, one would expect the presence of these two phases for the sample heated at 300 °C for 3 h, a fact which matches beautifully with the XRD analysis (see next section). Further heating of the precursor till 400 °C produces continuous intensity increase of the bands due to carbonate anion at the expense of those due to acetate one. The value of fraction decomposed, α, at 400 °C is 0.92 which is close to that expected for $Pr_2O_2(CO_3)$, $\alpha = 0.90$. Here, again, this value is in a good agreement with XRD analysis by confirming that the sample heated, at 400 °C for 3 h in air, composed mainly of the dioxycarbonate phase.

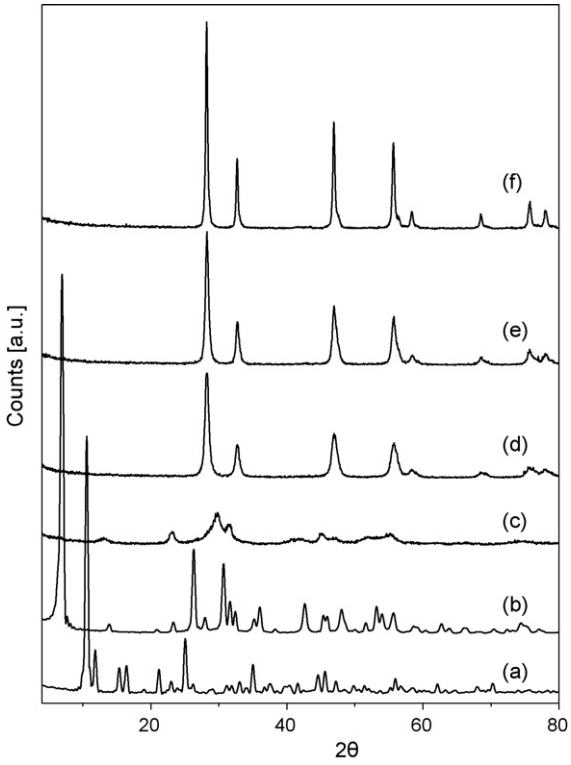

Fig. 6. XRD powder diffractograms obtained for the praseodymium acetate parent (a) and its calcination products at 300 °C (b), 400 °C (c), 500 °C (d), 600 °C (e), and 700 °C (f).

3.3. Characterization of the calcinations products of PrAc

3.3.1. X-ray diffraction

XRD patterns obtained for PrAc as well as its calcination products formed in air at the 300–700 °C temperature range are shown in Fig. 6. It is evident that heating the parent salt to 300 °C is accompanied by a noticeable change in the relevant XRD patterns. Our analysis showed that the Pr-300 sample (Fig. 6b) consists of two phases. The first one (minor phase) was identified to be $Pr_2O_2(CO_3)$ [ICDD No. 37-805]. The second phase (major), with reflections at $2\theta = 6.95$, 31.71, 32.49 and 36.10, did not matched with the ICDD data for hydrated or anhydrous acetates. In this respect, the IR spectra of the sample heated at 300 °C for 10 min (Fig. 5d) or that heated for 3 h (not shown) revealed the presence of absorptions due to acetate anion. Searching in the ICDD data bank reveals the absence of $Pr(OH)(CH_3COO)_2$ or $PrO(CH_3COO)$ cards. Accordingly, the obtained reflections could be related to the presence of acetate phase probably $PrO(CH_3COO)$, however, this suggestion needs further investigation. XRD diffractogram for Pr-400 sample (Fig. 6c) matched well with that reported for $Pr_2O_2(CO_3)$ [ICDD No. 25-696]. The detection of another phase of dioxycarbonate for the sample heated at 400 °C is in a good agreement with the reported work of Hussein [1] who assigned a phase transition $Pr_2O_2(CO_3)$ (I) to $Pr_2O_2(CO_3)$ (II) to occur exother-

Table 2
Texture data for the calcination products of praseodymium acetate

Calcination temperature (°C)	S_{BET} ($m^2\ g^{-1}$)	S_t ($m^2\ g^{-1}$)	V_p ($10^{-2}\ cm^3\ g^{-1}$)	Average pore diameter (Å)
300	12	14	2.7	403
400	19	25	4.3	415
500	17	23	4.1	407
600	16	23	4.2	402
700	10	10	2.1	406

mally at 390 °C during the DTA measurements. Moreover, he detected only $Pr_2O_2(CO_3)$ (II) for the sample heated in air, for 1 h, at 350 °C. Accordingly, the exothermic effects located at 370 °C in air and that at 409 °C in nitrogen (taking into account its broadness which extends from about 325 to 435 °C, Fig. 2), which was related to the decomposition of the salt and/or combustion of the volatile organic gases, can be also assigned to this phase transition. In other words, the peaks at 370 °C in air and that at 409 °C in nitrogen atmospheres are complex in nature and can be assigned to describe many simultaneous processes. XRD analysis of the samples heated at 500–700 °C illustrated the presence of $PrO_{1.833}$ [ICDD No. 6-329] as the only phase detected. Moreover, the peaks intensity increases with increasing the calcinations temperature indicating the increased crystallinity. In this context, the calculated crystallite sizes of $PrO_{1.833}$ for the samples heated at 500, 600, and 700 °C were found to be about 14, 17, and 30 nm, respectively.

3.3.2. Texture analysis

The surface characterization data are displayed in Table 2. Nitrogen sorption isotherms for the calcinations products of PrAc (Fig. 7) are of type II of Brunauer's classification [29,30]. The hysteresis loops are nearly of type H3. This suggests that the surface pores are slit-shaped or interplating [30]. The closure of the hysteresis loops for the samples calcined at temperatures ≥400 °C is shifter to higher relative pressure values with increasing the calcinations temperature which indicates the pore narrowing which results from sintering and agglomeration of the crystallites. This goes parallel with the XRD crystallite size analysis for the samples calcined at 500–700 °C range. Raising the calcination temperature from 300 to 400 °C is accompanied by marked increase in the surface area. This can be correlated with the weight change of the acetate parent as illustrated by thermal analysis and XRD results. Thus, the evolved gases together with the decomposition of the salt leading to the formation of dioxycarbonate are responsible for the creation of new system having the observed higher surface area. With further increase in the heating temperature produces a mild decrease in the measured surface areas till 600 °C and a sharp decrease for the sample calcined at 700 °C. This trend of variation could be attributed to two opposing effects: (i) evolution of CO_2 which expected to increase the surface areas, and (ii) sintering effect which leads to surface area decrease. Accordingly, it seems that the later effect predominates for the Pr-700 sample. On the whole, for all the samples studied, the S_t values obtained from the slope of the linear parts of the V_a–t plots (not shown) agrees satisfactorily with the corresponding S_{BET} values (Table 2). Meanwhile, the trend of variation of S_t values with the calcination temperature is similar to that exhibited by S_{BET} values.

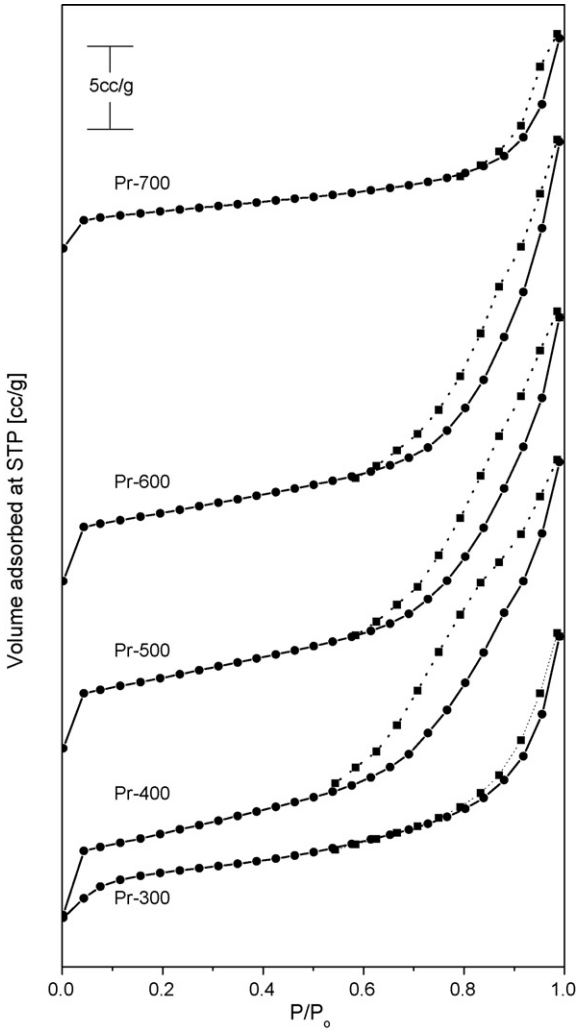

Fig. 7. Nitrogen sorption isotherms for the praseodymium acetate calcined at various temperatures.

4. Conclusions

Combining all the information collected from the present investigation led us to conclude the following points:

1. Thermal decomposition of PrAc proceeds with the formation of $Pr(OH)(CH_3COO)_2$, $PrO(CH_3COO)$, and $Pr_2O_2(CO_3)$ intermediates leading eventually to the formation of $PrO_{1.833}$.

Moreover, two different phases of praseodymium dioxycarbonate were detected as stable intermediates during the thermal genesis of $PrO_{1.833}$.

2. In conjunction with the results inferred from the thermal analysis, in situ electrical conductivity measurements provide an interesting technique to follow up the formation of the previously mentioned intermediates.
3. Texture analysis revealed that the 300–700 °C calcined samples exhibit a mesoporous nature. $PrO_{1.833}$ formed at 500 °C has a surface area of $17\,m^2\,g^{-1}$ and a crystallites size of 14 nm. The S_{BET} value drops to $10\,m^2\,g^{-1}$ whereas the crystallites size jump to 30 nm for $PrO_{1.833}$ obtained at 700 °C.

Acknowledgement

The authors would like to thank Prof. Dr. S. Weber (Pittsburg University, USA) for his generous donation of the praseodymium acetate sample used in this investigation.

References

[1] G.A.M. Hussein, J. Anal. Appl. Pyrolysis 29 (1994) 89–102.
[2] G.A.M. Hussein, J. Chem. Soc. Faraday Trans. 91 (1995) 1385–1390.
[3] M. Popa, M. Kakihana, Solid State Ionics 141–142 (2001) 265–272.
[4] G.A.M. Hussein, J. Anal. Appl. Pyrolysis 37 (1996) 111–149.
[5] I.S. Shaplygin, V.P. Komarov, V.B. Lazarev, J. Thermal. Anal. 15 (1979) 215–223.
[6] Y. Masuda, Thermochim. Acta 67 (1983) 271–285.
[7] G.A.M. Hussein, B.A.A. Balboul, M.A. A-Warith, A.G.M. Othman, Thermochim. Acta 369 (2001) 59–66.
[8] A.M. Wynne, J.E. Roberts, Thermochim. Acta 7 (1973) 159–171.
[9] P. Šulcová, M. Trojan, Thermochim. Acta 395 (2003) 251–255.
[10] S. Sugiyama, T. Miyamoto, H. Hayashi, M. Tanaka, J.B. Moffat, J. Mol. Catal. A 118 (1997) 129–136.
[11] K. Asami, K. Kusakabe, N. Ashi, Y. Ohtsuka, Appl. Catal. A 156 (1997) 43–56.
[12] J. Liu, Z. Zhao, A. Duan, L. Wang, S. Zhang, Catal. Commun. 8 (2007) 220–224.
[13] G.A.M. Hussein, J. Chem. Soc. Faraday Trans. 90 (1994) 3693–3697.
[14] B.M. Abu-Zied, Bull. Fac. Sci. Assiut Univ. B 31 (2) (2002) 23–38.
[15] G.A.M. Hussein, G.A.H. Mekhemer, B.A.A. Balboul, Phys. Chem. Chem. Phys. 2 (2000) 2033–2038.
[16] J. Hölsä, T. Turkki, Thermochim. Acta 190 (1991) 335–343.
[17] G.A.M. Hussein, H.M. Ismail, Bull. Chem. Soc. Jpn. 67 (1994) 2628–2634.
[18] P.R. Chapman, R.H. Griffith, J.D.F. Marsh, Proc. R. Soc. (London) 224 (1954) 419–426.
[19] B.C. Lippens, B.G. Linsen, J.H. de Boer, J. Catal. 3 (1964) 32–37.
[20] J.H. de Boer, B.C. Lippens, B.G. Linsen, J.C.P. Broekhoff, A. van den Heuvel, Th. J. Osinga, J. Colloid Sci. 21 (1966) 405–414.
[21] E.P. Barrett, L.G. Joyner, P.P. Halenda, J. Am. Chem. Soc. 73 (1951) 373–380.
[22] L.S. Birks, H. Friedman, J. Appl. Phys. 17 (1946) 687–692.
[23] M.H. Yao, R.J. Baird, F.W. Kunz, T.E. Hoost, J. Catal. 166 (1997) 67–74.
[24] G.A.M. Hussein, H. Ismail, Bull. Chem. Soc. Jpn. 67 (1994) 2634–2638.
[25] A.M. El-Awad, B.M. Abu-Zied, J. Mol. Catal. A 176 (2001) 213–226.
[26] A.K. Nikumbh, S.K. Pardeshi, M.N. Raste, Thermochim. Acta 374 (2001) 115–128.
[27] K. Nakamoto, Infrared Spectra of Inorganic and Coordination Compounds, Wiley, New York, 1970, p. 253.
[28] P. Bsraldi, Spectrochim. Acta 38A (1982) 51–55.
[29] P.A. Webb, C. Orr, Analytical Methods in Fine Particles Technology, Micromeritics Instrument Corp., 1997, p. 55.
[30] G. Leofanti, M. Padovan, G. Tozzola, B. Venturelli, Catal. Today 41 (1998) 207–219.